



Technical Note

Importance of nonequilibrium thermal conductivity during short-pulse laser-induced desorption from metals

Paul J. Antaki *

Antaki & Associates, Inc., P.O. Box 212, Howell, NJ 07731, USA

Received 12 February 2001; received in revised form 5 November 2001

1. Introduction

This work shows that using a nonequilibrium thermal conductivity for conduction electrons during short-pulse (e.g., 0.1 ps) laser heating of metals can be important for predicting laser-induced desorption of species from the metals.

To show the importance, this work extends the study of Phinney and Tien [1] that uses the equilibrium thermal conductivity for conduction electrons. Their study shows that during short-pulse heating desorption is driven mainly by high temperatures of conduction electrons at the surface of a metal. Also, they summarize previous studies of desorption induced by short-pulse lasers and discuss its growing number of applications. Ref. [2] provides a more recent status of laser-induced desorption.

Similar to [1], the work reported here uses the parabolic two-temperature model [3,4] to describe the behavior of conduction electrons and metal lattice. With this model, a short pulse of laser energy heats the electrons to temperature T_e , then the electrons transfer energy to the cooler lattice with temperature T_l . Hence for a short period of time after heating begins the electrons and lattice are not in thermal equilibrium because $T_e > T_l$. However, after enough time elapses they equilibrate so that $T_e = T_l$.

Ref. [5] solves the Boltzmann transport equation for conduction electrons and their interactions with the lattice to obtain the nonequilibrium thermal conductivity κ_{neq} of those electrons:

$$\kappa_{\text{neq}} = (T_e/T_l)\kappa_{\text{eq}} \quad (1)$$

where κ_{eq} , used in [1], is the conventional thermal conductivity of a metal obtained under equilibrium conditions ($T_e = T_l$). Eq. (1), used here, shows that $\kappa_{\text{neq}} > \kappa_{\text{eq}}$ during the nonequilibrium period because $T_e > T_l$ during this period. Refs. [5,6] discuss the approximations behind Eq. (1), and [6] cites another approach that leads to the equation.

Importantly, [7] shows that using κ_{neq} instead of only κ_{eq} leads to better agreement between temperature predictions and corresponding measurements for short-pulse laser heating. Consequently, predictions of desorption using κ_{neq} should be more accurate than predictions using only κ_{eq} because desorption is very sensitive to temperature, as noted later.

2. Desorption problem

Except for nonequilibrium conductivity, the desorption problem solved here is the same as in [1] where the front surface of a metal film with thickness L is subjected to a short pulse from a laser emitting visible light. Laser energy is absorbed within the film, heating it from initial temperature T_0 to temperatures that cause significant desorption of species from the front surface according to an Arrhenius model for desorption rate. Heat conduction in the film is one-dimensional in the direction of its thickness, and no heat exchange occurs between the front or back surface of the film and its surroundings. Also, the species attached to the front surface are transparent to the laser energy and the desorption process does not affect the electron and lattice temperatures. Consequently, these temperatures are determined with the two-temperature model, then desorption is calculated using these temperatures.

More generally, the other approximations adopted and discussed in [1] are retained here. For example, the

* Tel.: +1-732-919-7500.

E-mail address: antakip@asme.org (P.J. Antaki).

Nomenclature

| | |
|-------|--|
| A | scaling factor for desorption rate |
| C | heat capacity per unit volume |
| E | activation energy of desorption |
| G | electron–lattice (phonon) coupling factor |
| F | laser fluence per pulse |
| k | Boltzmann constant |
| L | film thickness |
| n | surface concentration of attached species |
| R | film reflectivity |
| RY | ratio of desorption yields, $\Delta\sigma_{\text{eq}}/\Delta\sigma_{\text{neq}}$ |
| t | time |
| t_p | FWHM duration of laser pulse |
| T | temperature |
| x | position |

Greek symbols

| | |
|--------------|---|
| β | dimensionless activation energy, E/kT_0 |
| Γ | dimensionless parameter, $Gt_p/\gamma T_0$ |
| γ | coefficient of electronic heat capacity per unit volume |
| $\Delta\eta$ | dimensionless space step |

| | |
|----------------|---|
| $\Delta\sigma$ | dimensionless desorption yield, $\sigma_0 - \sigma$ |
| $\Delta\tau$ | dimensionless time step |
| δ | radiation penetration depth |
| ϵ | dimensionless parameter, L/δ |
| η | dimensionless position, x/L |
| θ | dimensionless electron temperature, T_e/T_0 |
| κ | thermal conductivity of conduction electrons |
| Λ | dimensionless parameter, $2(\ln 2)^{1/2}F(1-R)/\pi^{1/2}\delta\gamma T_0^2$ |
| λ | dimensionless parameter, $\kappa_{\text{eq}}t_p/\gamma L^2 T_0$ |
| μ | dimensionless parameter, $\gamma T_0/C_1$ |
| σ | dimensionless surface concentration, n/At_p |
| τ | dimensionless time, t/t_p |
| φ | dimensionless lattice temperature, T_l/T_0 |

Subscripts

| | |
|-----|----------------|
| e | electron |
| eq | equilibrium |
| l | lattice |
| neq | nonequilibrium |
| 0 | initial |

scaling factor A for desorption rate in the Arrhenius model is identical for contributions to desorption from electron and lattice temperatures. Also, the transparency of species means they are not directly heated by the laser. Ref. [1] discusses conditions for which this transparency, as well as the Arrhenius desorption model, are reasonable approximations. Although the problem involving the direct heating of species by the laser is beyond the scope of the work reported here, it is useful to note that Ref. [2] discusses this problem.

The two-temperature model with nonequilibrium conductivity is obtained here by incorporating Eq. (1) from this work into Eqs. (1) and (2) from [1]. Cast in dimensionless form for generality the model is

$$\theta \frac{\partial \theta}{\partial \tau} = \lambda \frac{\partial}{\partial \eta} \left(\frac{\theta}{\varphi} \frac{\partial \theta}{\partial \eta} \right) - \Gamma(\theta - \varphi) + \Lambda \exp[-\epsilon\eta - (4 \ln 2)\tau^2] \quad (2)$$

$$\partial \varphi / \partial \tau = \mu \Gamma(\theta - \varphi) \quad (3)$$

with boundary and initial conditions:

$$\frac{\partial \theta}{\partial \eta}(0, \tau) = 0 \quad (4a)$$

$$\frac{\partial \theta}{\partial \eta}(1, \tau) = 0 \quad (4b)$$

$$\theta(\eta, -5) = 1 \quad (5a)$$

$$\varphi(\eta, -5) = 1 \quad (5b)$$

Here, the electron and lattice temperatures are $\theta(\eta, \tau)$ and $\varphi(\eta, \tau)$, respectively, τ is the time, η the position in the film, and λ , Γ , Λ , ϵ and μ are parameters.

The first term on the right-hand side of Eq. (2) accounts for electron diffusion including the effect of non-equilibrium conductivity represented by θ/φ . The last term on the right-hand side of this equation represents laser heating described by the time-variation of a Gaussian pulse centered (peaking) at $\tau = 0$ with a full width at half maximum (FWHM) pulse duration [8]. However, Eqs. (5a) and (5b) state the initial time as $\tau = -5$ because the Gaussian “tail” for $\tau < -5$ contains a negligible amount of energy [1].

Eq. (5) in [1] is the Arrhenius model for the rate of desorption from the front surface. In dimensionless form that model and an initial condition are

$$-d\sigma/d\tau = \exp(-\beta/\theta_{\eta=0}) + \exp(-\beta/\varphi_{\eta=0}) \quad (6)$$

$$\sigma(-5) = \sigma_0 \quad (7)$$

where $\sigma(\tau)$ is the concentration of species on the front surface of the film and β the activation energy of desorption. In Eq. (6) just stated, the electron and lattice temperatures are those values at the front surface $\eta = 0$ where desorption occurs. Integrating Eq. (6) gives the dimensionless desorption yield $\Delta\sigma$ resulting from laser heating.

The desorption problem with nonequilibrium conductivity stated by Eqs. (2)–(7) reduces to the problem with equilibrium conductivity by setting $\theta/\varphi = 1$ in the first term on the right-hand side of Eq. (2).

3. Effect of nonequilibrium conductivity

The effect that nonequilibrium conductivity can have on desorption is shown here by comparing desorption yields predicted using equilibrium and nonequilibrium conductivities for single crystal, defect-free gold films with thicknesses of 50, 75, 100 and 2000 nm. All these films, initially at 300 K, are subjected to the laser pulse duration and fluence per pulse of $t_p = 0.1$ ps and $F = 100$ J/m² [1], respectively. Using the properties for gold from Table 2 in [1], all films have the common values of $\Gamma = 0.13$, $\Lambda = 71.71$ and $\mu = 8.00 \times 10^{-3}$ because these parameters do not involve film thickness. With the parameters that depend on thickness, for the 50 nm film: $\lambda = 0.63$ and $\epsilon = 3.27$; 75 nm film: $\lambda = 0.28$ and $\epsilon = 4.90$; 100 nm film: $\lambda = 0.16$ and $\epsilon = 6.54$; 2000 nm film: $\lambda = 3.94 \times 10^{-4}$ and $\epsilon = 130.72$. Further, the range of dimensionless activation energy is $\beta = 15$ –65 based on the range of E cited in [1]. More specifically, this range of β corresponds approximately to E ranging from 0.4 to 1.7 eV, respectively. Also, temperatures and desorption yields are calculated over the same time period as in [1] of -0.5 to 50.0 ps, or $\tau = -5.0$ to 500.0 for the dimensionless time used here.

The temperature problem stated by Eqs. (2)–(5b) was solved numerically using central difference and forward difference approximations for space and time derivatives, respectively. After solving this problem for equilibrium and nonequilibrium cases, the desorption yields were calculated by integrating Eq. (6) with the trapezoidal rule. After that, the ratio of desorption yields RY was formed by dividing the yield obtained with equilibrium conductivity, $\Delta\sigma_{eq}$, by the yield obtained with nonequilibrium conductivity, $\Delta\sigma_{neq}$, so $RY = \Delta\sigma_{eq}/\Delta\sigma_{neq}$.

The stability criterion [9] relating time step $\Delta\tau$ to space step $\Delta\eta$ was $\Delta\tau < \Delta\eta^2/2\lambda$ for this temperature problem with derivative boundary conditions. In rigorous terms this criterion applies only to linear homogeneous problems, but it is a reliable criterion here, as is often the case for nonlinear problems [9]. To obtain converged values of temperatures and desorption yields, space and time steps were reduced in size until changes of <1% would occur in calculated values with smaller step sizes. For example, with the 100 nm film these step sizes were $\Delta\eta = 2 \times 10^{-3}$ and $\Delta\tau = 1 \times 10^{-5}$. The temperature calculations were tested by confirming temperatures obtained in [5] and [10] with the nonequilibrium conductivity, as well as in [1] and [4] using only the equilibrium conductivity. Finally, the desorption calculations were tested by confirming the desorption yields of [1] obtained for equilibrium conductivity.

In the results discussed next, film thicknesses are cited for convenience despite the adoption of dimensionless terms for Eqs. (2)–(7). The discussion focuses on conditions at the front surface of the film because desorption occurs there.

3.1. Electron temperatures

Fig. 1 shows electron temperatures at the front surface of the 100 nm film during $\tau = -2.0$ to 8.0 for the cases of nonequilibrium and equilibrium conductivities. Although the laser pulse is taken to begin at $\tau = -5.0$, the smallest time shown is $\tau = -2.0$ to approximate the time when the pulse begins to noticeably increase electron temperatures. To establish reference points in the figure, it is noted that the approximate maximum values of electron temperature $\theta = 8.3$ and 6.3 for the equilibrium and nonequilibrium cases, respectively, correspond to actual temperatures of about 2490 and 1890 K using the initial temperature of 300 K (for which $\theta = 1$). Lattice temperatures are not shown because they experience much smaller increases and have a negligible effect on desorption [1].

The key feature of Fig. 1 is that nonequilibrium conductivity reduces the electron surface temperature compared to the temperature obtained with only equilibrium conductivity. This reduction is a consequence of the larger conductivity for the nonequilibrium case, noted previously with Eq. (1), implying that electrons carry more energy away from the surface region than in the equilibrium case.

Although the laser pulse peaks at $\tau = 0$, Fig. 1 shows that electron temperatures for both cases continue to increase for short periods after this time because the laser still provides energy faster than electrons carry it away from the surface region. However, this period is shorter for the nonequilibrium case because its larger thermal conductivity leads to greater energy removal from the surface region, as just noted. While not shown in the figure, electron temperatures for the two cases eventually converge because the final temperature of the film is the same for each case.

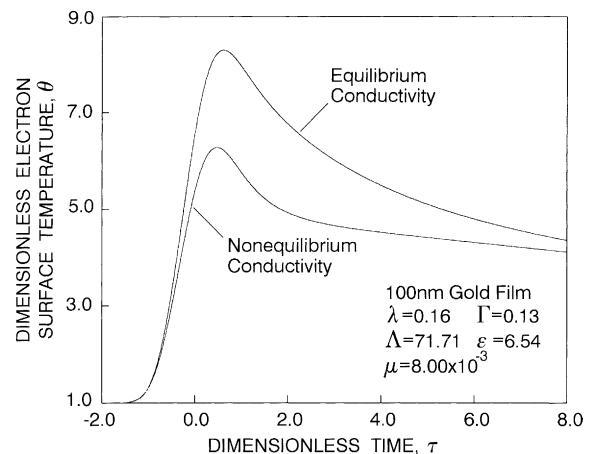


Fig. 1. Comparison of transient electron temperatures at front surface of film for cases of equilibrium and nonequilibrium thermal conductivities of electrons.

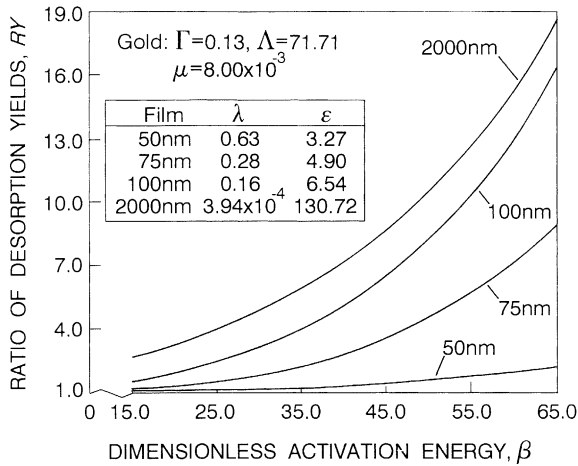


Fig. 2. Behavior of desorption yield ratio as a function of activation energy of desorption and film thickness.

More generally, the reduction in electron surface temperature just attributed to nonequilibrium conductivity with the 100 nm film also occurs with the other film thicknesses (not shown).

3.2. Desorption yields

Fig. 2 shows the ratio of desorption yields RY as a function of activation energy of desorption β , for each film thickness. More specifically, the figure shows that $RY > 1$ over the entire range of β and film thickness. Consequently, using only the equilibrium conductivity overpredicts desorption yield relative to the nonequilibrium case because $RY = \Delta\sigma_{eq}/\Delta\sigma_{neq}$.

The figure shows this overprediction by the equilibrium case tends to be large for the t_p and F used here except for a relatively small set of activation energies and film thicknesses (e.g., $\beta = 15$ and $L = 50$ nm). Hence, using the nonequilibrium conductivity can have an important effect on predictions of desorption. This importance stems from electron surface temperatures that are lower than those obtained using only the equilibrium conductivity, as noted previously for Fig. 1. In turn, these lower temperatures can dramatically reduce the rate of desorption because its Arrhenius model, given by Eq. (6), is very sensitive to electron temperature through the exponential term involving this temperature.

Also, Fig. 2 shows that for constant film thickness, RY increases as β increases. This increase in RY results from the behaviors of desorption yields $\Delta\sigma_{eq}$ and $\Delta\sigma_{neq}$ as β increases. In particular, the term $\exp(-\beta/\theta_{\eta=0})$ (the “Boltzmann factor”) in Eq. (6) is proportional to the fraction of attached species that possess energy β , which is the minimum energy required for desorption. Thus, as

β increases both yields decrease because there are fewer species with enough energy to desorb. However, qualitatively studying a plot (e.g., [11]) of the Boltzmann energy distribution shows that at the lower temperatures of the nonequilibrium case, the fraction of species with enough energy to desorb decreases more rapidly as β increases compared to the equilibrium case. Consequently, $\Delta\sigma_{neq}$ decreases more rapidly than $\Delta\sigma_{eq}$, causing RY to increase because $RY = \Delta\sigma_{eq}/\Delta\sigma_{neq}$.

In the limit $\beta \rightarrow 0$, $RY \rightarrow 1$ because temperature no longer affects desorption as shown by Eq. (6) when the Boltzmann factors converge to 1 for each case. Thus in this limit the desorption yields become identical functions of dimensionless time τ .

In addition, Fig. 2 shows that at constant β , RY increases as film thickness increases. Again, the behaviors of $\Delta\sigma_{eq}$ and $\Delta\sigma_{neq}$ cause this increase in RY: as film thickness increases, both yields decrease because of reduced electron surface temperatures (the same amount of laser energy is deposited into thicker films) but $\Delta\sigma_{neq}$ decreases faster than $\Delta\sigma_{eq}$, leading to the increase in RY. This faster decrease in $\Delta\sigma_{neq}$ occurs because an increasing film thickness permits electrons to diffuse further from the surface region, lowering the temperature there [1]. Accordingly, the larger conductivity and corresponding increased diffusion of electrons for the nonequilibrium case cause greater reductions in temperature and accompanying desorption yield relative to the equilibrium case.

Interestingly, the increase in RY just noted for increasing film thickness does not continue indefinitely. In fact, the maximum thickness used in Fig. 2 is 2000 nm because, at about this value, further increases in thickness do not cause additional changes in RY. Thus the values of RY at 2000 nm are its upper bounds for the t_p and F used here. More specifically, this 2000 nm film is sufficiently thick that the temperature at the back surface remains at its initial value during the time period covered by the desorption calculations. In effect, the presence of the back surface does not influence temperatures at the front surface during the calculations. Further, even if this time period were extended, the surface temperature would be too low to cause additional desorption and RY would again remain unchanged.

In contrast to the maximum thickness just noted, the minimum value of thickness used in Fig. 2 is 50 nm because “size effects” such as the influence of film thickness on thermal conductivity become important at about this value [12], but accounting for these effects is beyond the scope of this work. Qualitatively, however, it is expected that RY would approach 1 over the entire range of β as film thickness continuously decreases below 50 nm. This expectation arises from the increasingly uniform temperature profiles that would accompany decreasing thickness [1], minimizing the role of

thermal conductivity by reducing the importance of electron diffusion.

Finally, although not shown here, $RY > 1$ for the other values of t_p and F considered in [1]. And similar to the behavior shown in Fig. 2, using only equilibrium conductivity to predict desorption with these other values can cause a significant overprediction of desorption yield relative to the yield obtained with nonequilibrium conductivity.

In conclusion, the importance of nonequilibrium thermal conductivity shown here suggests that it should be used for predicting desorption from metals induced by short-pulse lasers when desorption follows an Arrhenius model.

References

- [1] L.M. Phinney, C.L. Tien, Electronic desorption of surface species using short-pulse lasers, *J. Heat Transfer* 120 (1998) 765–771.
- [2] E. Gerhard, Dynamics of reactions at surfaces, in: B.C. Gates, H. Knözinger (Eds.), *Advances in Catalysis*, vol. 45, Academic Press, New York, 2000, pp. 1–69.
- [3] S.I. Anisimov, B.L. Kapeliovich, T.L. Perelman, Electron emission from metal surfaces exposed to ultrashort laser pulses, *Sov. Phys. JETP* 39 (1974) 375–377.
- [4] T.Q. Qiu, C.L. Tien, Short-pulse laser heating of metals, *Int. J. Heat Mass Transfer* 35 (1992) 719–725.
- [5] T.Q. Qiu, C.L. Tien, Heat transfer mechanisms during short-pulse laser heating of metals, *J. Heat Transfer* 115 (1993) 835–841.
- [6] P.B. Corkum, F. Brunel, N.K. Sherman, T. Srinivasan-Rao, Thermal response of metals to ultrashort-pulse laser excitation, *Phys. Rev. Lett.* 61 (1988) 2886–2889.
- [7] T.Q. Qiu, Energy dissipation and transport during high-power and short-pulse laser-metal interactions, Ph.D. Thesis, University of California, Berkely, CA, 1993, pp. 83–84.
- [8] J.P. Longtin, C.L. Tien, Microscale radiation phenomena, in: C.L. Tien, A. Majumdar, F.M. Gerner (Eds.), *Microscale Energy Transport*, Taylor and Francis, Washington, DC, 1998, p. 128.
- [9] R.H. Pletcher, W.J. Minkowycz, E.M. Sparrow, G.E. Schneider, Overview of basic numerical methods, in: W.J. Minkowycz, E.M. Sparrow, G.E. Schneider, R.H. Pletcher (Eds.), *Handbook of Numerical Heat Transfer*, John Wiley and Sons, Inc., New York, 1988, p. 71.
- [10] T.Q. Qiu, C.L. Tien, Femtosecond laser heating of multilayer metals. I. Analysis, *Int. J. Heat Mass Transfer* 37 (1994) 2789–2797.
- [11] K. Wark, *Thermodynamics*, third ed., McGraw-Hill, New York, 1976, p. 432.
- [12] T.Q. Qiu, C.L. Tien, Size effects on nonequilibrium laser heating of metal films, *J. Heat Transfer* 115 (1993) 842–847.